

Effects of Fibre Volume Fraction on the Compressive and Flexural Experimental Behaviour of SFRC

Lidia Rizzuti

Department of Civil Engineering
McMaster University, Hamilton, Ontario, Canada

Francesco Bencardino

Department of Civil Engineering
University of Calabria, Rende, Cosenza, Italy

Copyright © 2014 Lidia Rizzuti and Francesco Bencardino. This is an open access article distributed under the Creative Commons Attribution License, which permits unrestricted use, distribution, and reproduction in any medium, provided the original work is properly cited.

Abstract

The purpose of this study is to analyse the effects of fibre volume fraction on the mechanical properties of SFRC (Steel Fibre Reinforced Concrete). The results obtained from compression and four-point bending tests carried out on concrete specimens with fibre volume fraction of 1%, 1.6%, 3% and 5% are critically examined. The experimental behaviour in terms of peak load, post-peak behaviour, and residual strength, are evaluated and compared. The fibre distribution and their contribution in Mode I fracture is also assessed. The effects of steel fibre volume fraction on the strength, ultimate strain and ductility index of SFRC are highlighted in order to give a guide for structural use.

Keywords: Mechanical Properties, Steel Fibre Reinforced Concrete, Strength

1. Introduction

Fibre Reinforced Concrete (FRC) is a cementitious composite material whose behaviour is improved by means of the activation of fibre pull-out mechanism after the cracking of the matrix and it is characterized by a residual tensile strength. The mechanical behaviour of this material depends on the fibre amount, the fibre geometry, the fibre orientation, the fibre dispersion, the cementitious matrix mix design, and the concrete placement (Swamy and Mangat, 1974; Yazici,

Inan and Tabok, 2007; Bencardino et al. 2008; Alani and Aboutalebi, 2013; Bencardino et al. 2013). Usually, steel fibres with high modulus are used to improve mechanical properties whereas low modulus fibres such as polypropylene can reduce cracking due to shrinkage and control spalling phenomena in concrete (Sasikala and Vimala, 2013). In addition, it needs to be emphasized that the correlation between fibre distribution, fresh and hardened-state properties of FRC are also important when designing enhanced cement composites for structural uses (Ferrara and Meda, 2006).

The structural design based on the use of FRC requires the knowledge of the mechanical and fracture properties at their hardened state. The complex interaction between all these parameters suggests to consider the composite as a unique material whose mechanical features have to be identified by means of suitable tests.

Test procedure for evaluating the compressive behaviour is harmonized, whereas, this does not apply to the experimental procedure for evaluating the tensile post-cracking behaviour and toughness indexes. The most common test setup is the bending test carried out on unnotched or notched specimens that have to reproduce the real conditions of the structure. Two types of configurations have been recommended by the main standards such as the three-point bending tests (EN 14651, 2007) and the four-point bending test (UNI 11039-1, 2003; UNI 11039-2, 2003; ASTM C1609/C1609M, 2012). Both the European and the Italian standard suggest the use of notched specimens while the American Standard recommend prismatic specimens without notch.

Moreover, the recent guidelines CNR-DT 204 (2007) and fib Model Code (2010) proposed, for structural design and analysis of Steel Fibre Reinforced Concrete (SFRC) members, stress-opening and stress-strain relationship in uniaxial tension identified by means of bending tests, referring the Italian guideline to the UNI Standard and the European Code to the EN Standard.

In order to evaluate the effects of fibre volume fraction on the performance of SFRC a set of compression tests on cylinder samples and four-point bending tests on prismatic notched specimens were carried out. The effect of steel fibre volume fraction on the main mechanical parameters as peak load, peak stress, and post-peak response were analysed in compression and in tension. The dispersion of the steel fibres on the specimen's fracture surface was also evaluated for estimating the consistency and its effects on the mechanical tensile parameters.

2. Test programme

Specimens

The experimental investigation was carried out on cylinder samples and notched prisms of plain concrete (PC) and SFRC. The steel fibre volume fraction were 1%, 1.6%, 3% and 5%. In each group the specimens were labelled by means of a set of letters (PC = ordinary-concrete; S1%, S1.6%, S3%, S5% = reinforced-concrete with 1%, 1.6%, 3%, 5% of steel fibre volume fraction) followed by the number of

the specimen. Three tests were carried out for each concrete mix and specimen size for a total number of 15 cylinder samples (compression test) and 15 notched prisms (four-point bending test).

Materials, concrete mix design, casting and curing

The following components were used: Portland cement ASTM type I, crushed coarse aggregates, quartz sand, water, condensed silica fume and superplasticizer. The maximum size of the coarse aggregates was 15 mm. The steel fibres have hooked ends, a tensile strength of 350-400 MPa, a length of 22 mm, and an aspect ratio of 40. Table 1 shows the PC, and SFRC (S1%, S1.6%, S3% and S5%) composition for 1 m³ of concrete batch.

Table 1. Mixture proportion – per cubic meter of concrete.

Material	Symbol	Unit	PC	SFRC			
				S1%	S1.6%	S3%	S5%
Cement	c	kg		500			
Quartz	0-2 mm	kg		377			
	3-6 mm			273			
Aggregate	10-15 mm	kg		317			
	5-10 mm			290			
	0-5 mm			693	615	567	458
Fibre	-	kg	-	78	126	235	392
	V _f	%	0	1	1.6	3	5
Silica fume	sf	kg		30			
	sf/c	%		6			
Superplasticizer	sp	kg		7.5			
	sp/c	%		1.5			
Water	w	l		175			
	w/c	%		35			

Plain concrete was designed for a 28 days cylinder strength of 60 MPa. In order to obtain a cohesive and flowable mix and a uniform fibre distribution, gap-grading of the aggregates was avoided. When fibres were added to the mix, the same weight of 0-5 mm coarse aggregate was removed to keep the same fineness modulus. The mixes were prepared by using a conventional mixer. The prismatic specimens were cast by filling the moulds according to UNI 11039-2 (2003), and then were vibrated on a shaking table. All test specimens were removed from the moulds after 24 hours and were cured for 28 days under water saturated sand.

Test procedure and instrumentation

The uniaxial compression tests were carried out at 28 days on 150 mm x 300 mm cylinders, according to EN 12390-3 (2009). A Zwick/Roell servo hydraulic closed-loop test machine with a capacity of 3000 kN was used. The loads were increased at a rate of 0.05 mm/min. Three HBM WA20 LVDTs (Linear Variable

Displacement Transducers) with a gauge length of 100 mm were used to measure strains on the cylindrical samples. They were mounted at 120-degree intervals on a circular tie placed on the cylinder surface at 100 mm from the top of the sample. A second tie was placed on the sample at 100 mm from the bottom and provided the reaction frame for the three LVDTs. Each tie was made of two aluminium half rings connected by springs. These aluminium ties were able to support the measuring devices, to allow lateral deformations when they occurred, and did not give confinement effect on the samples under loading. Figure 1 shows a cylindrical sample with the position of the instrumentation.

The bending tests were carried out at 28 days on 150 mm x 150 mm x 600 mm prismatic specimens, according to UNI 11039-2 (2003). A single notch with a depth of 45 mm was sawn at mid-span to allow the crack to localize. The displacement rate of the crosshead testing machine was 0.05 mm/min. A 100 kN INSTRON 1195 electromechanical testing machine fitted up with a 100 kN C1 HBM load cell was used. The vertical displacement was measured, with reference to the load points, by means of two LVDTs placed along the front and back faces of each specimen. The transducers were fixed to a rigid yoke in order to minimize the effect of the rotations during the test. Furthermore, two LVDTs were placed at the notch tip on the two faces of the specimen to measure Crack-Tip Opening Displacement (CTOD). The Crack-Mouth Opening Displacement (CMOD) was measured as well, by a TML resistive full bridge transducer astride the notch. In all tests, data acquisition and signal control were carried out by using an HBM Spider 8 control unit. The four-point bending setup is shown in Figure 2.



Fig. 1. Compressive test setup.



Fig. 2. Bending test setup.

3. Test results and analysis

Compressive strength

The compressive strength test results are summarized in Table 2.

Table 2. Uniaxial compression strength.

Material	Specimens	Mean strength value, MPa
Plain Concrete	PC	66.7
Steel Fibre Reinforced Concrete	S1%	69.6 (+4.35%)
	S1.6%	68.2 (+2.25%)
	S3%	65.8 (-1.35%)
	S5%	61.7 (-7.50%)

This table shows the mean value calculated on three samples for each group and the difference percentage of compressive strength respect to the ordinary concrete. Test results show that the experimental compressive strength value of the ordinary concrete is 66.7 MPa greater than 60 MPa, as defined in the design stage. The concrete obtained has a high compressive strength and could be classified as High Performance Concrete (HPC). The addition of fibres in this high strength concrete matrix, compared to the ordinary concrete matrix, affects the compressive peak strength value only slightly but influences the post-peak response in a more positive way. Specifically, SFRC with low fibre volume fraction showed a slight increase of the peak compressive strength, 4.35% for $V_f = 1\%$ and 2.25% for $V_f = 1.6\%$, respectively. In the case of SFRC with medium-high fibre volume fraction ($V_f = 3\%$ and 5%) a slight decrease of the peak compressive strength was detected. A slight decrease of 1.35% for SFRC with $V_f = 3\%$ and a decrease of 7.50% for SFRC with $V_f = 5\%$, respectively. The typical stress-strain curves for PC and SFRC cylinders loaded in uniaxial compression are given in Figure 3.

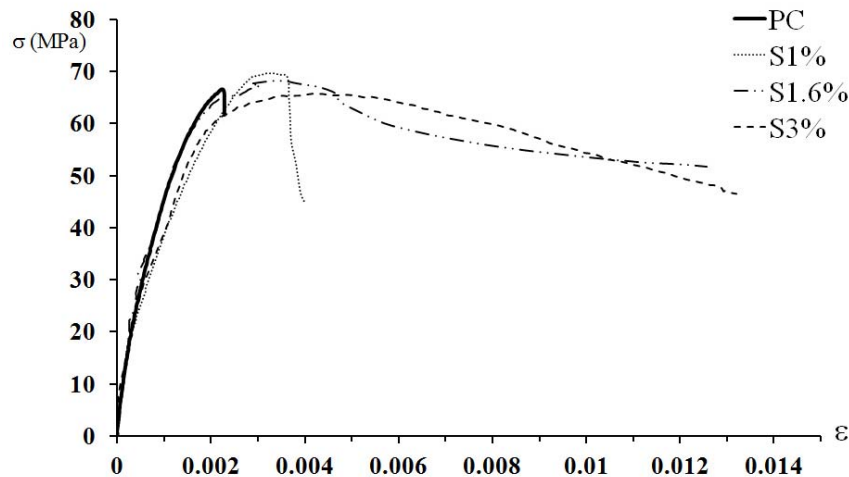


Fig. 3. Typical stress-strain compression curves.

Concrete reinforced with a low content of steel fibres ($V_f = 1\%$) shows only a minor improvement in the descending or softening branch of the stress-strain curve compared to plain concrete. Concrete reinforced with fibre content higher than 1% show a more extended softening branch. The ultimate strain, reached values of 0.012 to 0.014 for SFRC with 1.6% and 3% of fibre volume fraction, about five times the ultimate strain of plain concrete. It is worthwhile to note that

at a strain of 0.01 the SFRC with 1.6% and 3% of fibre content have a residual stress of about 80% of their peak stress.

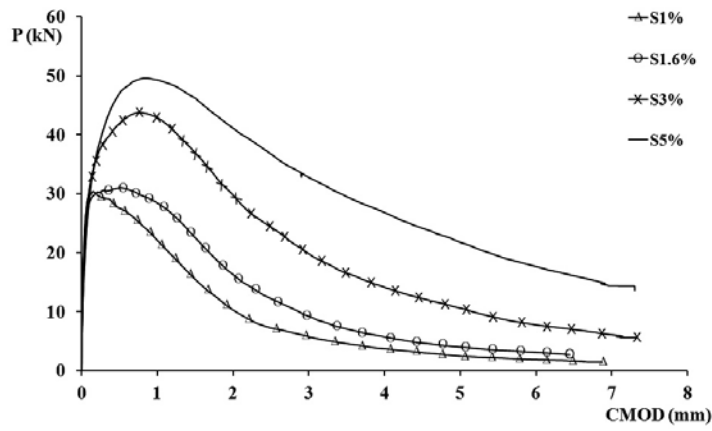
These results highlight that the most predominant role of steel fibres is to modify the failure mode of HPC from a brittle failure to a more ductile failure pattern. The post-test aspects of the failed specimens showed that, in the case of plain concrete, either a single shear plane or a cone-type failure occurred. By contrast, SFRC specimens showed a large number of longitudinal cracks near the failure zone, which were oriented in the parallel or nearly parallel direction to the applied compressive stresses.

Bending tests and tensile strength parameters

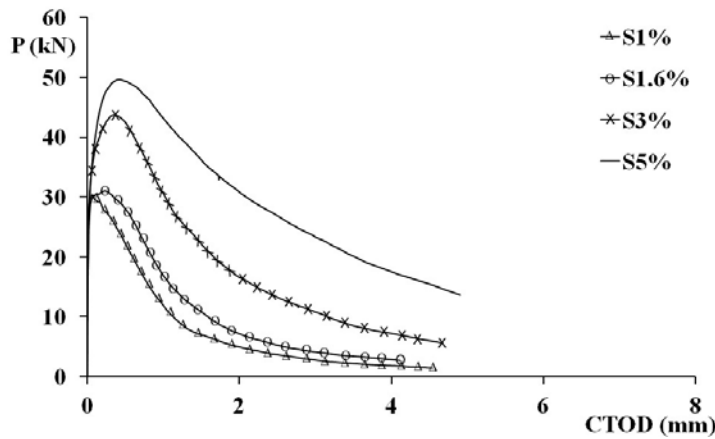
The behaviour of PC specimens was linear-elastic up to failure; thereafter the complete separation of each specimen into two parts occurred. The load-CMOD, load-CTOD, and load-deflection curves of the SFRC specimens are shown in Figures 4a, 4b, and 4c, respectively. CTOD values are the average values between the front and rear measurements. The SFRC curves typically show a linear branch up to first cracking point. Close to the peak load, there is stable crack propagation because of the favourable effects that the fibres have on the ligament. Beyond the peak load, there is a mechanical decay that is more or less pronounced depending on fibre volume fraction. As micro cracks coalesce into macro cracks, hooked-end fibres become increasingly efficient in crack bridging. The larger the fibre content, the higher the peak load. In fact, concrete specimens with low content of steel fibre ($V_f = 1\%$ and 1.6%) showed an increase of about 19-20% while in those with higher content ($V_f = 3\%$ and 5%) the increase is about of 72-95%, compared to PC specimens. The residual load evaluated at the CTOD value of 3 mm is about 9%, 13%, 11% and 47% of the peak load for $V_f = 1\%$, 1.6% , 3% and 5% , respectively.

These results make it possible to directly compute the fracture energy, as the area underneath the load-deflection curve or indirectly from the load-crack opening displacement curve. To obtain comparable results, the long softening branch should be truncated at a defined point. The area under the load-deflection curve was evaluated by referring to a limit displacement value of 3.00 mm. In this case the fracture energy is higher by about 48% in the case of medium content of fibre ($V_f = 1.6\%$) and it is two and 2.5 times higher for high fibre content ($V_f = 3\%$ and 5%) compared to SFRC with 1% of steel fibre volume fraction.

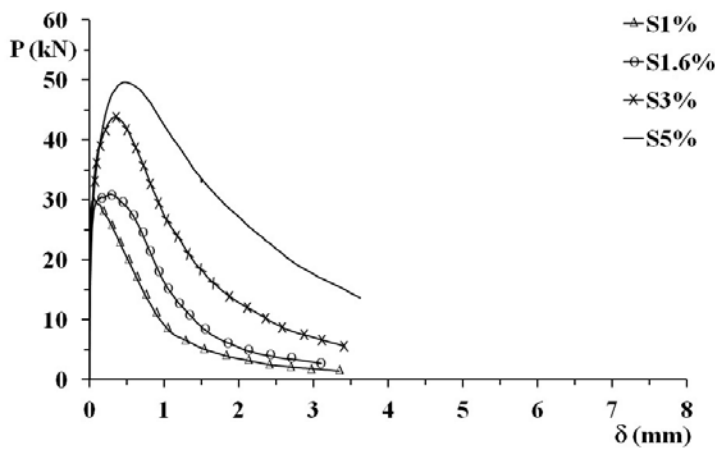
According to UNI 11039-2 (2003), the following parameters have to be evaluated in order to characterize the flexural tensile behaviour of SFRC: the load (P_{I_f}) and the strength (f_{I_f}) at first cracking, the equivalent strengths ($f_{eq(0-0.6)}$, $f_{eq(0.6-3)}$) and the ductility indexes (D_0 , D_I).



(a)



(b)



(c)

Fig. 4. Typical curves of SFRC specimens under four-point bending:
 (a) load-CMOD; (b) load-CTOD; (c) load-deflection.

The nominal strength at first cracking represents the behaviour of the cementitious matrix and, according to UNI 11039-2 (2003), can be computed by means of the expression:

$$f_{lf} = \frac{P_{lf} l}{b(h - a_0)^2} \quad (\text{MPa})$$

Where b (150 mm), h (150 mm), l (450 mm) are the width, height and span of the specimen, respectively; a_0 (45 mm) is the depth of the notch; and P_{lf} is the value of the load recorded for a Crack-Tip Opening Displacement equal to $CTOD_0$. The parameters $f_{eq(0-0.6)}$ and $f_{eq(0.6-3)}$ are the average nominal stresses in the $CTOD$ range between 0 and 0.6 mm, and in the range between 0.6 mm and 3 mm, respectively. These two parameters are the post-cracking equivalent strengths to be used at the serviceability limit state and at the ultimate limit state, respectively. These parameters can be computed by using the following relationships:

$$f_{eq(0-0.6)} = \frac{l}{b(h - a_0)^2} \frac{U_1}{0.6} \quad f_{eq(0.6-3)} = \frac{l}{b(h - a_0)^2} \frac{U_2}{2.4}$$

Where U_1 and U_2 should be evaluated from the following expressions:

$$U_1 = \int_0^{0.6} P(CTOD) d(CTOD) \quad U_2 = \int_{0.6}^3 P(CTOD) d(CTOD)$$

The ductility indexes can be calculated by:

$$D_0 = \frac{f_{eq(0-0.6)}}{f_{lf}} \quad D_1 = \frac{f_{eq(0.6-3)}}{f_{eq(0-0.6)}}$$

All these equations were formulated by assuming a linear distribution for the stresses acting on the cross section at mid-span. The values of the above parameters are given in Table 3. The load and strength values at first cracking are similar for each fibre volume fraction. The equivalent strengths $f_{eq(0-0.6)}$ and $f_{eq(0.6-3)}$, and the ductility indexes D_0 and D_1 increase when fibre volume fraction increases.

Fibre dispersion on fracture surface

In order to evaluate the effect of fibre dispersion in the matrix on the mechanical performance of SFRC, as governed by the fresh state properties of concrete through the casting process, per each of the four mixes described the fracture surface of the notched prismatic specimens was ideally divided in four rows and five columns cells (Figure 5). For each type of SFRC (1%, 1.6%, 3%, and 5%) the average number of fibres on the fracture surface of the three tested specimens was calculated. The comparison of fibre dispersions is given in Figure 6. The fibre dispersion for each type of SFRC are shown in Figure 7a, 7b, 7c, and 7d. Quite uniform fibre dispersion were obtained without a pronounced fibre percentage in the casting direction. In the case of FRC with very high steel fibres volume fraction ($V_f = 5\%$) the steel fibres were more densely packed on the layer of casting surface compared to the central layers. This is due to the fact that during the casting of the specimen the time required for vibration was not enough for the high dosage of the fibre in the mixture which led to a slightly not homogeneous distribution of the fibres.

Table 3. Flexural tensile parameters of SFRC.

Specimen	P_{lf} kN	f_{lf} MPa	$f_{eq(0-0.6)}$ MPa	$f_{eq(0.6-3)}$ MPa	D_0 -	D_1 -	Specific n° fibres/cm ²
S1%_1	24.6	6.7	7.1	2.0	1.1	0.3	0.67
S1%_2	25.5	6.9	5.3	1.8	0.8	0.3	0.69
S1%_3	24.5	6.7	5.5	1.2	0.8	0.2	0.65
Mean value	24.9	6.8	6.0	1.7	0.9	0.3	0.67
S1.6%_1	20.3	5.5	7.9	2.8	1.4	0.4	1.02
S1.6%_2	20.1	5.5	7.7	2.8	1.4	0.4	1.21
S1.6%_3	22.4	6.1	7.4	2.6	1.2	0.4	1.08
Mean value	20.9	5.7	7.7	2.7	1.3	0.4	1.10
S3%_1	24.1	6.6	15.1	8.7	2.3	0.6	2.58
S3%_2	30.6	8.3	11.0	4.8	1.3	0.4	2.20
S3%_3	24.5	6.7	11.2	5.7	1.7	0.5	2.04
Mean value	26.4	7.2	12.4	6.4	1.8	0.5	2.27
S5%_1	25.4	6.9	12.8	8.3	1.9	0.6	3.71
S5%_2	18.9	5.1	12.4	9.3	2.4	0.8	3.92
S5%_3	16.3	4.4	10.6	5.2	2.4	0.5	3.45
Mean value	20.2	5.5	11.9	7.6	2.2	0.6	3.69

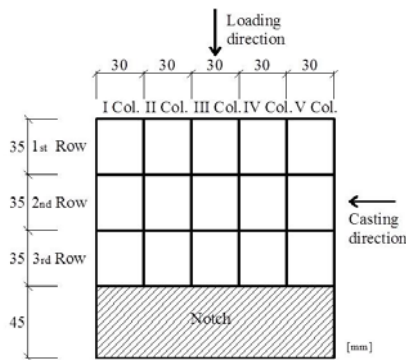


Fig. 5. Fracture surface discretization.

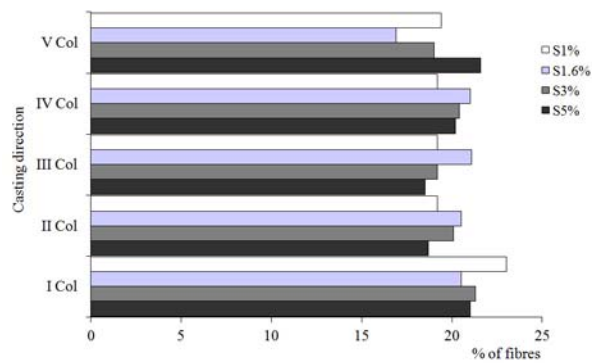


Fig. 6. Comparison of fibre dispersion on fracture surface.

A uniform crack opening on the two faces of the specimens was developed. As it was expected, the number of fibres on the fracture surface increased with the content of fibres, Figure 8 (a). The first cracking and the post-cracking equivalent stresses were plotted versus the number of the fibres on the fracture surface, Figure 8 (b). The post-cracking equivalent strengths show a quite linear relationship with the fibres content while the first crack strengths exhibit an almost constant relationship. As it was expected, the number of fibres on the fracture surface increased with the content of fibres, Figure 8 (a). The first cracking and the post-cracking equivalent stresses were plotted versus the number of the fibres on the fracture surface, Figure 8 (b). The post-cracking equivalent strengths show a quite linear relationship with the fibres content while the first crack strengths exhibit an almost constant relationship.

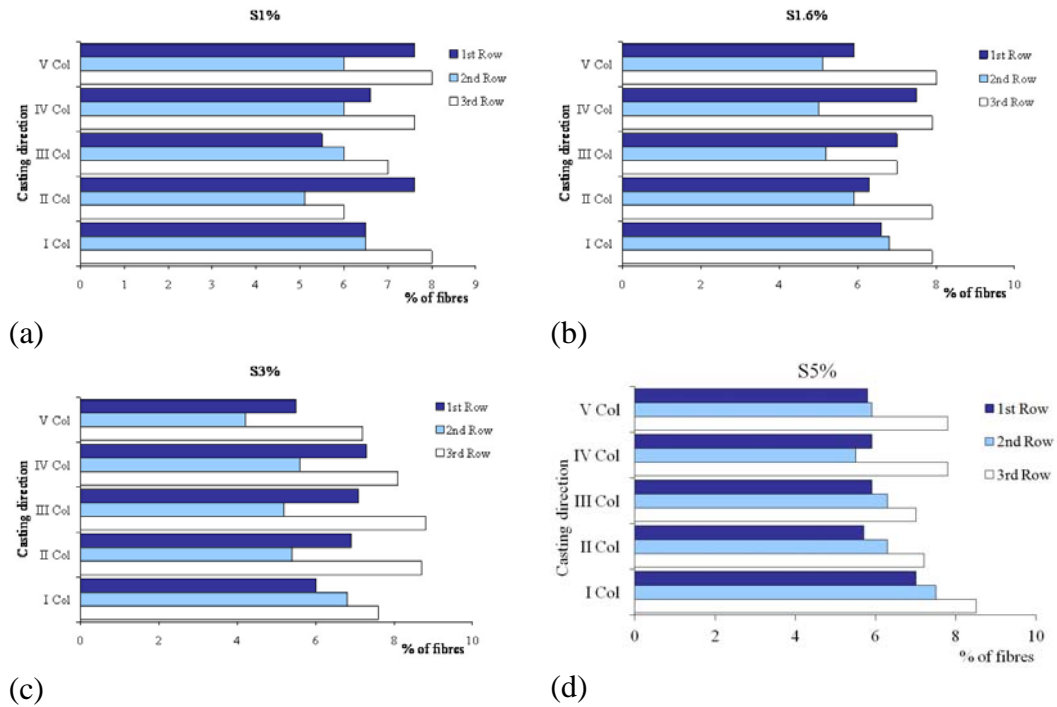


Fig. 7. Fibre dispersion on fracture surface of each SFRC type.

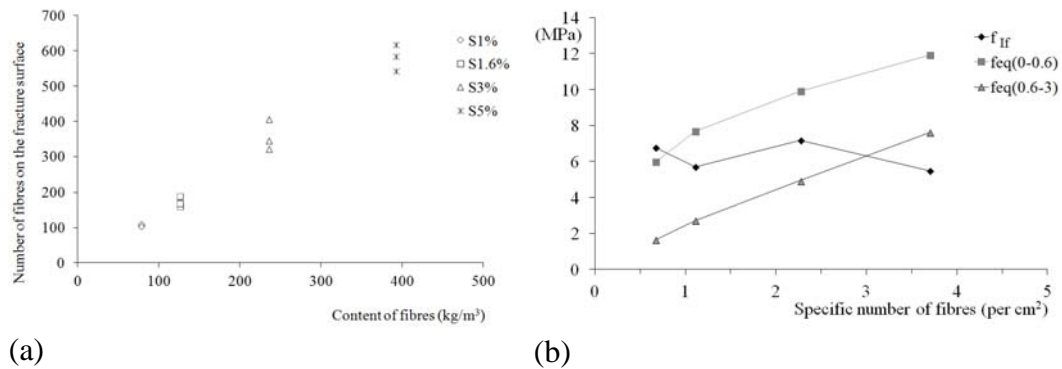


Fig. 8. Relationship between: (a) content vs. number of fibres; (b) specific number of fibres vs. tensile strength parameters.

4. Conclusions

The following conclusions can be drawn from this investigation:

- The addition of fibres does not significantly affect the compressive strength of concrete. The increase in fibre content improves the post-peak behaviour and a more extended softening branch is observed.
- SFRC specimens with fibre volume fraction of 1.6% and 3% show, at 0.01 strain, a residual compressive stress of about 80% of their respective peak stresses. At these fibre volumes, the ultimate strain at failure reaches values of three to five times the ultimate strain values fixed by current guidelines.

- The use of medium-high steel fibres contents significantly improves the post-peak behaviour in tensile for flexure, by extending the softening branch and reducing the negative slope.
- Steel fibres give to the concrete a sizable post-peak residual strength. The residual load evaluated at the CTOD value of 3 mm is about 9%, 13%, 11% and 47% of the peak load for fibre content of 1%, 1.6%, 3% and 5%, respectively. This lead to an improved fracture energy and toughness of SFRC materials with high fibre content compared to ordinary concrete.
- The data obtained emphasize that, through correct mix design, consistent quality of fibre concrete with high strength and high fibre volume fraction can be manufactured and placed in the field.
- The mechanical properties of SFRC with medium-high fibre content suggest the use of such material for many structural applications, with and without traditional internal reinforcement. The use of SFRC is, thus, particularly suitable for structures when they are subjected to loads over the serviceability limit state in bending and shear, and when exposed to impact or dynamic forces, as they occur under seismic or cyclic action.

References

- [1] Alani A.M. and Aboutalebi M., “Mechanical properties of fibre reinforced concrete - A comparative experimental study”, *International Journal of Civil, Architectural Science and Engineering World Academy of Science, Engineering and Technology*, **7(9)** (2013), 203-208.
- [2] ASTM C1609/C1609M: Standard test method for flexural performance of fiber-reinforced concrete (using beam with third-point loading), ASTM International, (2012), West Conshohocken, PA, United States.
- [3] Bencardino F., Rizzuti L., Spadea G. and Swamy R.N., “Stress-Strain behavior of steel fiber-reinforced concrete in compression”, *Journal of Materials in Civil Engineering*, **20(3)** (2008), 255-263.
- [4] Bencardino F., Rizzuti L., Spadea G. and Swamy R.N., “Implications of test methodology on post-cracking and fracture behaviour of Steel Fibre Reinforced Concrete”, *Composites Part B: Engineering*, **46** (2013), 31-38.
- [5] CNR-DT 204: Guide for the design and construction of fiber-reinforced concrete structures, National Research Council, Advisory Committee on Technical Recommendations for Construction, (2007), Rome, Italy.
- [6] EN 12390-3: Testing Hardened Concrete - Compressive Strength of Test Specimens, European Committee for Standardization, (2009AC:2011), Brussels.

- [7] EN 14651: Test method for metallic fibre concrete - Measuring the flexural tensile strength (limit of proportionality (LOP), residual). European Committee for Standardization, (2007), Brussels.
- [8] Ferrara L. and Meda A., “Relationships between fibre distribution, workability and the mechanical properties of SFRC applied to precast roof elements”, *Materials and Structures*, **39** (2006), 411-420.
- [9] fib Model Code: Model code for concrete structure - Bulletin 65. Fédération Internationale du Béton Lausanne, (2010), Switzerland.
- [10] Yazici S., Inan G. and Tabok V., “Effect of aspect ratio and volume fraction of steel fiber on the mechanical properties of SFRC”, *Construction and Building Materials*, **1(6)** (2007), 1250-1253.
- [11] Sasikala K. and Vimala S., “A comparative study of polypropylene, recron and steel fiber reinforced engineered cementitious composites”, *International Journal of Engineering Research & Technology*, **2(4)** (2013), 1136-1142.
- [12] Swamy R.N. and Mangat P.S., “Influence of fiber geometry on the properties of steel fiber reinforced concrete”, *Cement and Concrete Research*, **4** (1974), 451-456.
- [13] UNI 11039-1: Steel Fibre Reinforced Concrete - Definitions, Classification and Designation. National Italian Unification centre, (2003), Italy.
- [14] UNI 11039-2: Steel Fibre Reinforced Concrete - Test Method for Determination of First Crack Strength and Ductility Indexes. National Italian Unification centre, (2003), Italy.

Received: February 23, 2014